

Supplementary material

Characterization, oxidative desulfurization performance evaluation and catalytic reaction mechanism of polyoxometalate-coated, semi-encapsulated heart-shaped metal organic frameworks

Zhengxiang Sun,^a Rui Wang,^{*a}

^a School of Environmental Science and Engineering, Shandong University, No.27 Shanda South Road, Jinan 250199, PR China. *E-mail: wangrui@sdu.edu.cn (R. Wang).

1. Figures

Fig. S1. SEM image of H-POMOF, where the H-POMOF complex with a distinct semi-encapsulated style is labelled within the yellow dashed circle.

Fig. S2. TEM image of H-POMOF from 1 μm to 200 nm.

Fig. S3. SEM mapping of P, W, C and O elements of H-POMOF.

Fig. S4. Delamination occurred when the medium was left to stand at the end of the ODS reaction.

Fig. S5. (a) BET Surface Area Plot, (b) Langmuir Surface Area Plot and (c) t-Plot (Harkins and Jura) of H-POMOF.

Fig. S6. Illustrations of the heart-shaped MOF (H-MOF) from different perspectives after DFT structure optimization.

Fig. S7. Front view and van der Waals spheres morphology of the heart-shaped MOF (H-MOF) after DFT structure optimization.

Fig. S8. The label diagram, Polygon diagram, Ring diagram, and Van der Waals Spheres diagram of POM.

Fig. S9. Illustration of the (a) LUMO and (b) HOMO of POM.

Fig. S10. EDX spectrum analysis of H-POMOF composite material.

Fig. S11. Schematic diagram of electron transfer and metal oxidation state in the ODS catalytic reaction of H-POMOF.

2. Tables

Table S1 Elemental composition and atomic mass obtained by SEM mapping.

Table S2 Mesoporous BET related parameters of H-POMOF.

Table S3 Energy values and changes from the initial state (POM, H_2O_2) to the transition state (POM- H_2O_2) to the final state (POM-OH).

Table S4 Representative synthetic strategies and characteristics of POMOF-based materials.

Table S5 Comparison of oxidative desulphurisation performance of recently reported representative POMOF matrix composites.

Table S6 Langmuir adsorption isotherm parameters at 50°C.

Table S7 Langmuir adsorption isotherm parameters at 60°C.

Table S8 Langmuir adsorption isotherm parameters at 70°C.

Table S9 Adsorption thermodynamic parameters at 50°C.

Table S10 Adsorption thermodynamic parameters at 60°C.

Table S11 Adsorption thermodynamic parameters at 70°C.

Table S12 Cartesian Coordinates (A.U.) of POM by DFT.

Table S13 Mayer Population Analysis of POM by DFT.

3. References

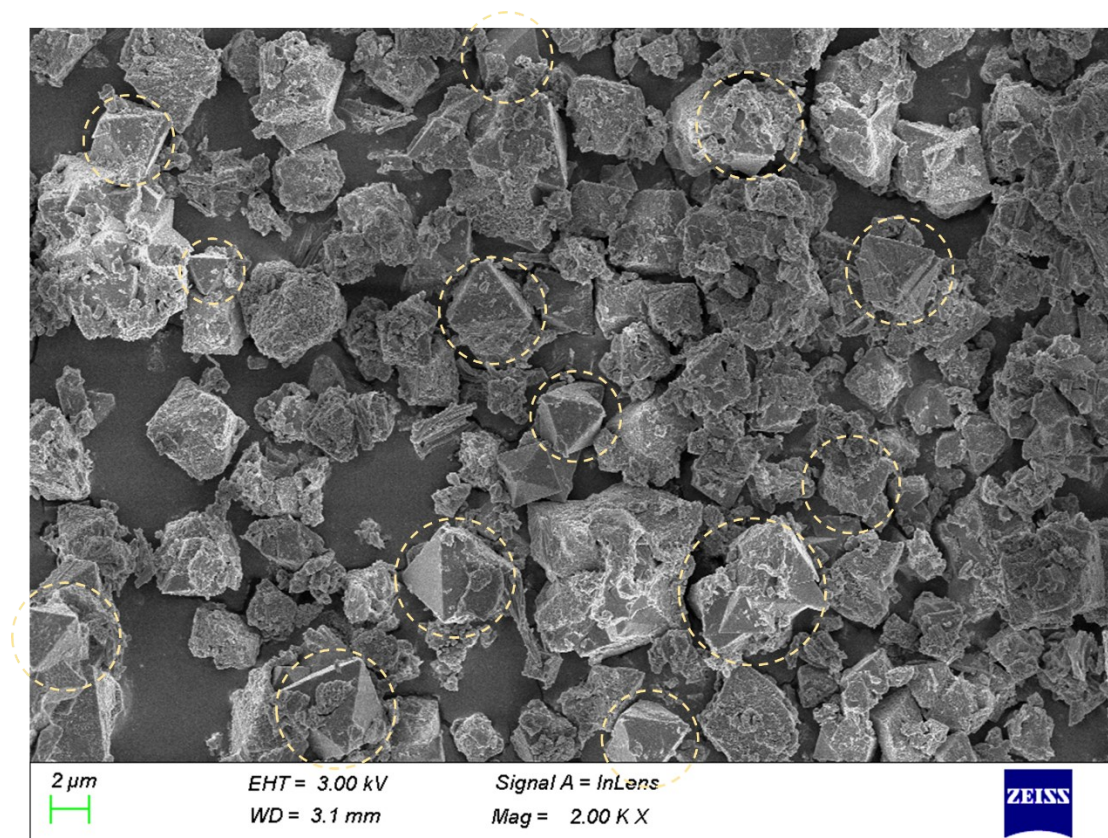


Fig. S1. SEM image of H-POMOF, where the H-POMOF complex with a distinct semi-encapsulated style is labelled within the yellow dashed circle.

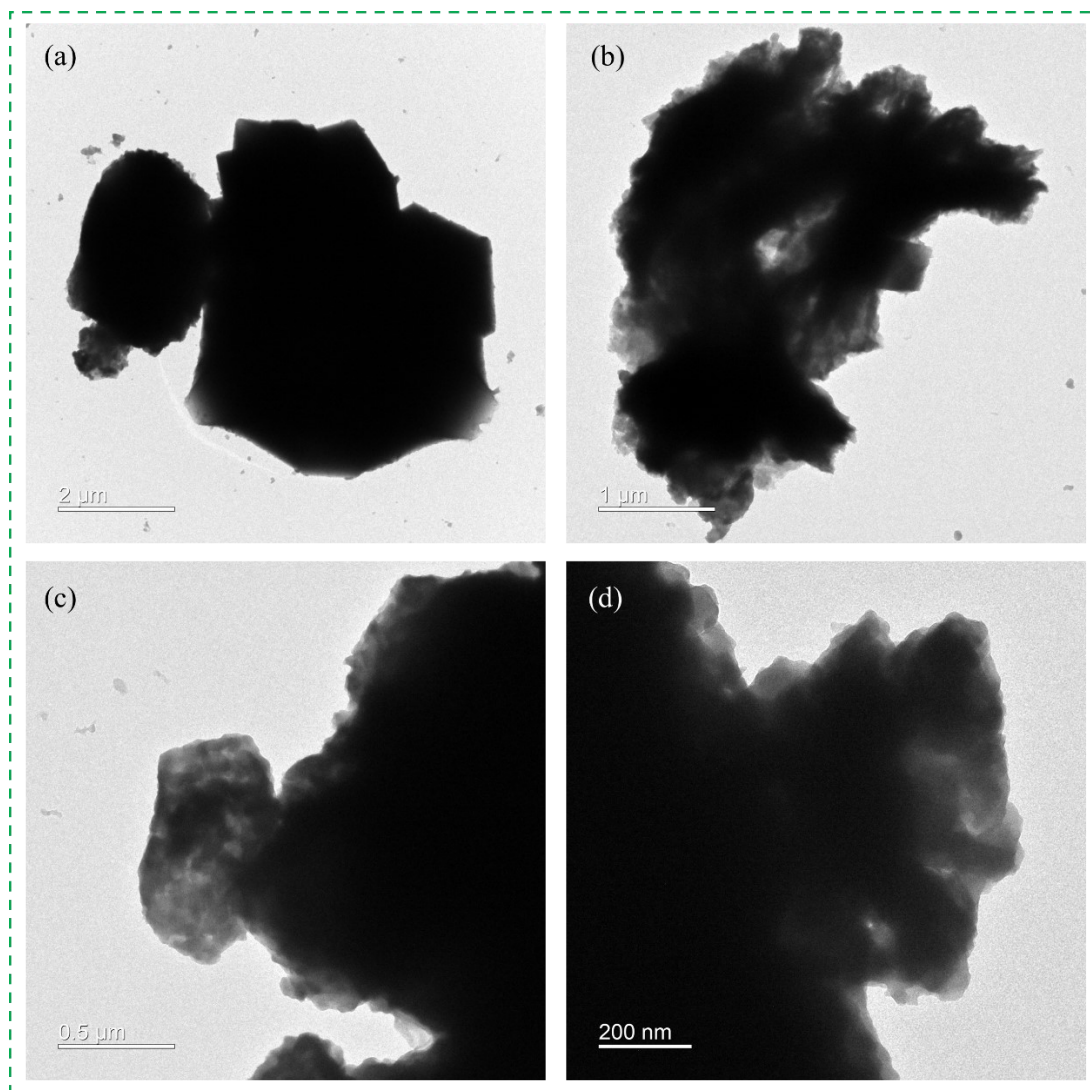


Fig. S2. TEM image of H-POMOF from 1 μm to 200 nm.

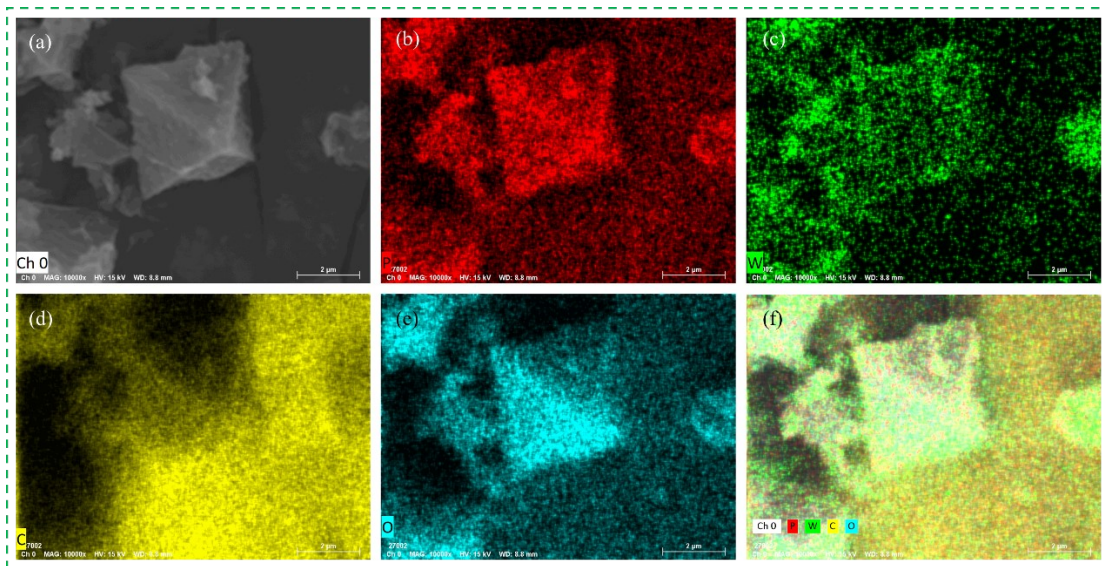


Fig. S3. SEM mapping of P, W, C and O elements of H-POMOF.

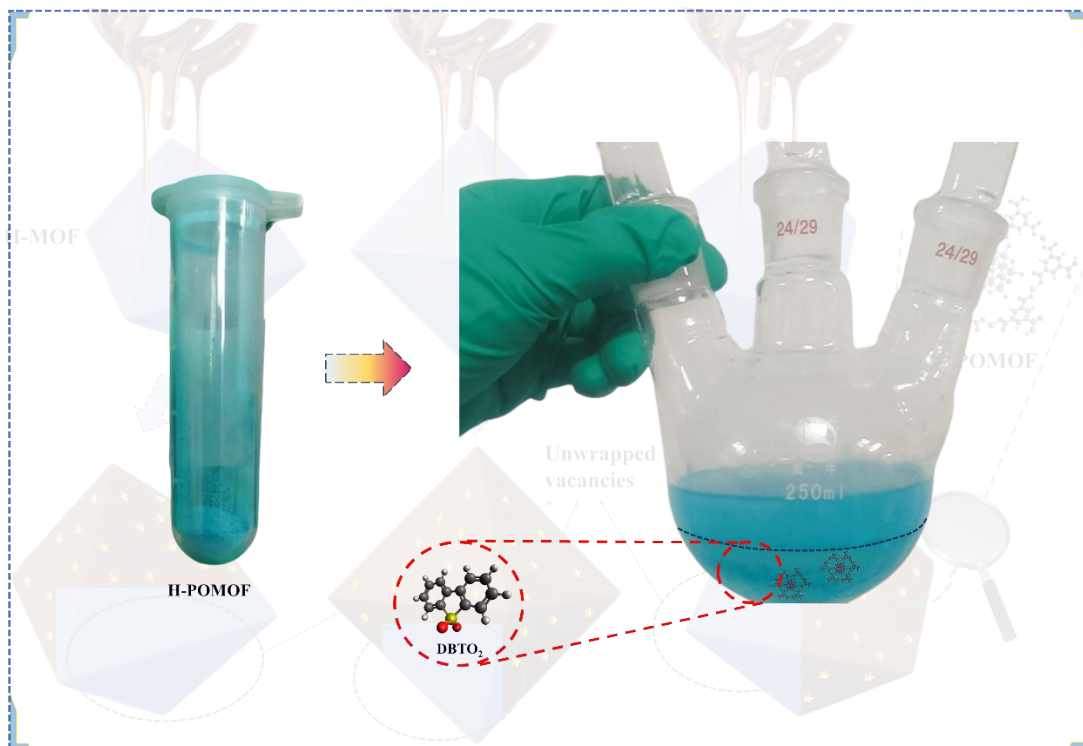


Fig. S4. Delamination occurred when the medium was left to stand at the end of the ODS reaction.

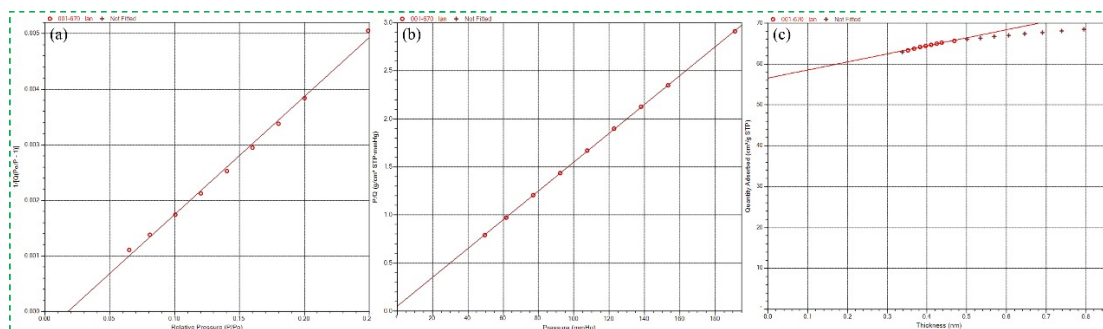


Fig. S5. (a) BET Surface Area Plot, (b) Langmuir Surface Area Plot and (c) t-Plot (Harkins and Jura) of H-POMOF.

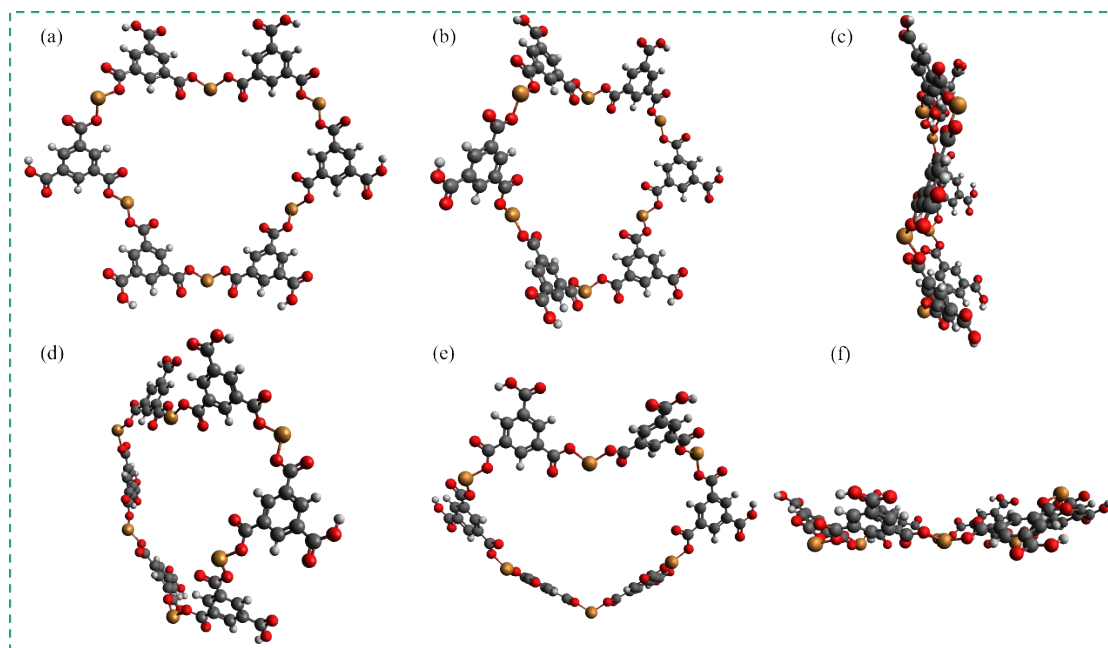


Fig. S6. Illustrations of the heart-shaped MOF (H-MOF) from different perspectives after DFT structure optimization.

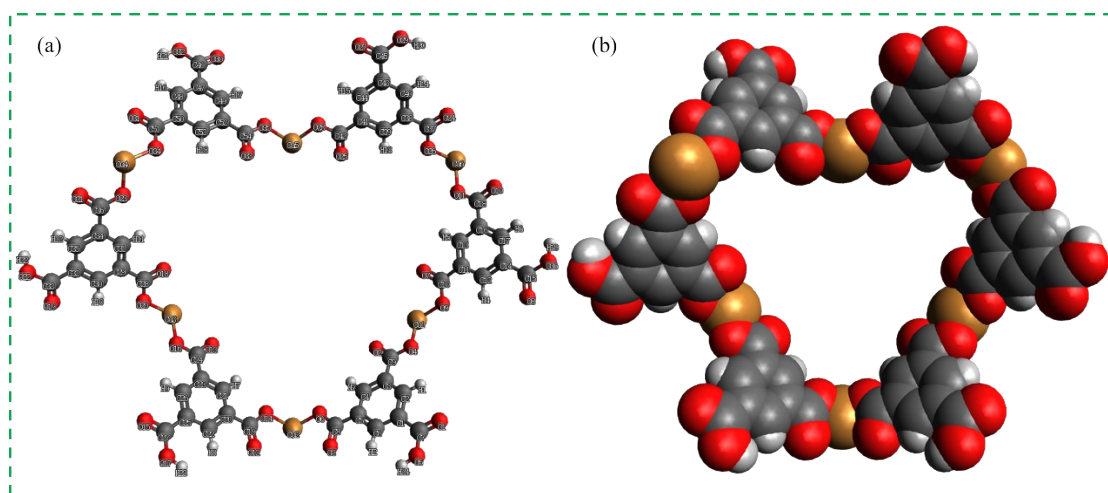


Fig. S7. Front view and van der Waals spheres morphology of the heart-shaped MOF (H-MOF) after DFT structure optimization.

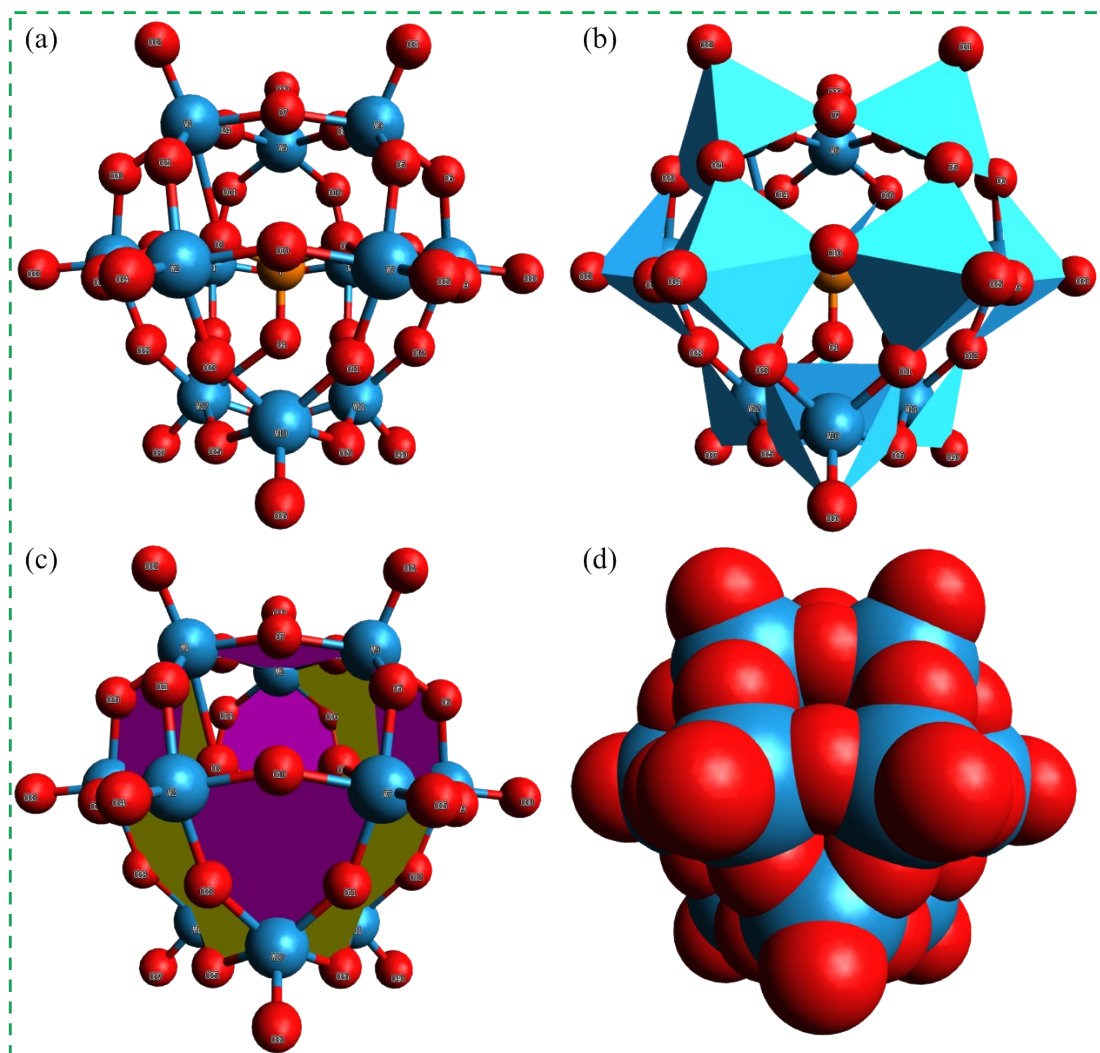


Fig. S8. The label diagram, Polygon diagram, Ring diagram, and Van der Waals Spheres diagram of POM.

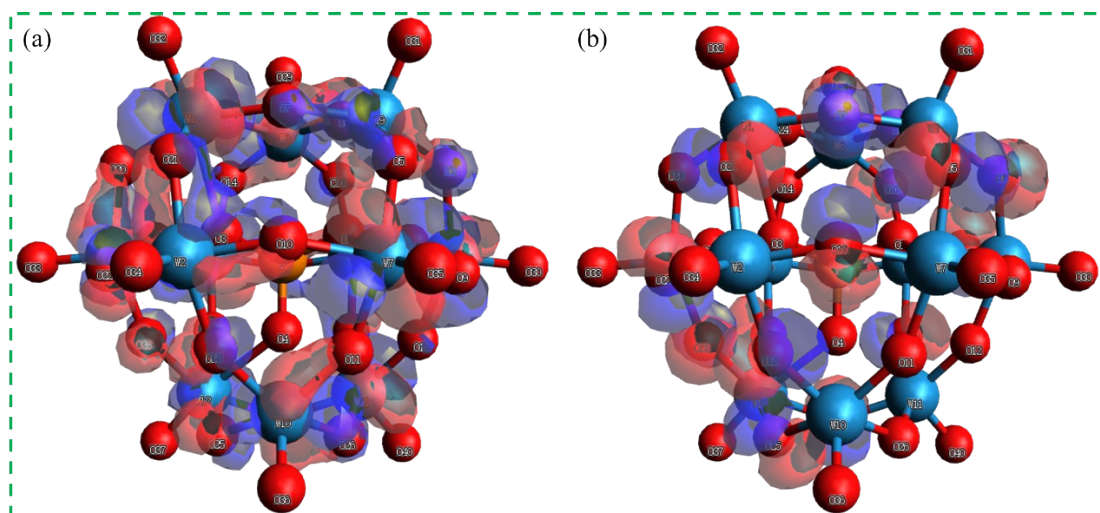


Fig. S9. Illustration of the (a) LUMO and (b) HOMO of POM.

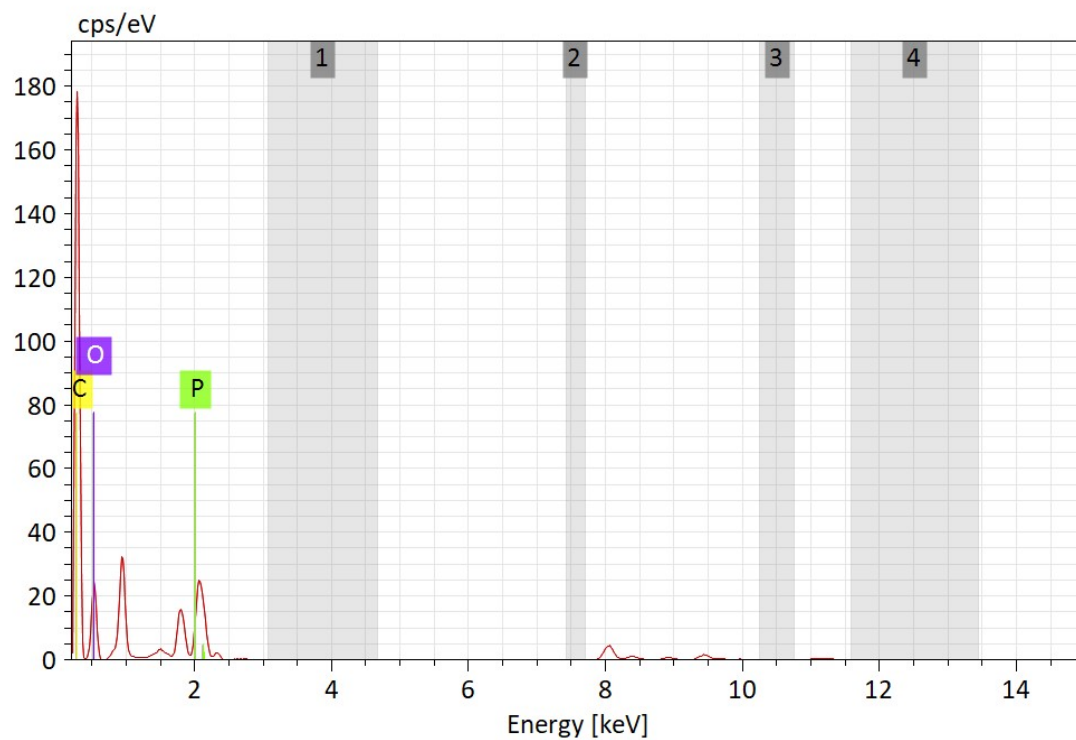


Fig. S10 EDX spectrum analysis of H-POMOF composite material.

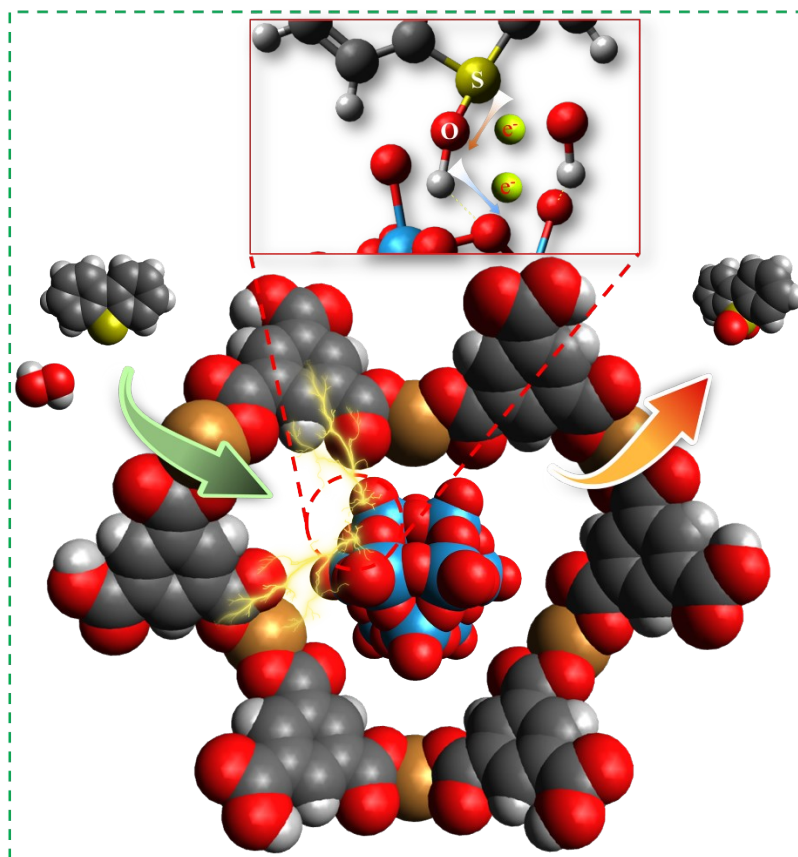


Fig. S11 Schematic diagram of electron transfer and metal oxidation state in the ODS catalytic reaction of H-POMOF.

Table S1 Elemental composition and atomic mass obtained by SEM mapping.

Elements	Atomic number	net worth	Mass (%)	Normalized quality	Atom	Abs. error (%)	Abs. error (%) (3 sigma)	rel. error (%) (3 sigma)
C	6	362611	29.50	71.54	82.02	3.15	9.44	31.99
O	8	53057	7.54	18.29	15.74	0.89	2.66	35.21
P	15	57935	1.65	3.99	1.78	0.06	0.19	11.49
W	74	4545	2.55	6.18	0.46	0.10	0.30	11.70
Total			41.24	100.00	100.00			

Table S2 Mesoporous BET related parameters of H-POMOF.

Surface Area		Pore Volume		Pore Size	
Single point surface area at $P/P_0 = 0.24929862$ 4:	214.5538 m ² /g	Single point adsorption total pore volume	0.125631 cm ³ /g	Adsorption average pore diameter	2.4065 nm
BET Surface Area:	208.8232 m ² /g	t-Plot micropore volume	0.132558 cm ³ /g	Desorption average pore diameter	2.5391 nm
Langmuir Surface Area:	290.1607 m ² /g	BJH Adsorption cumulative volume	0.048298 cm ³ /g	BJH Adsorption average pore diameter	9.4722 nm

Table S3 Energy values and changes from the initial state (POM, H₂O₂) to the transition state (POM-H₂O₂) to the final state (POM-OH).

State	Final single point energy (Hartree)	Δ Energy (Hartree)	ΔE (kcal/mol)
POM · H ₂ O ₂	-4309.4716	0	0
POM-H ₂ O ₂	-4309.1159	0.3557	223.2
POM-OH	-4309.499	-0.3831	-240.4

Table S4 Representative synthetic strategies and characteristics of POMOF-based materials.

POMOFs	POM	MOF	Diameter of porous cage (Å)	Organic ligands (linkers)	Synthetic methods	Application	Ref.
POM@ZIF-67	$H_3PW_{12}O_{40} \cdot 18H_2O$	ZIF-67	11.6	2-methylimidazole	Encapsulation	Photocatalytic water splitting	1
$(CH_3NH_2CH_3)[Cu_2(TPB)_2(PW_{12}O_{40})] \cdot 4DMF \cdot 6H_2O$	$H_3PW_{12}O_{40}$	–	12	1,2,4,5-tetra(4-pyridyl)benzene (TPB)	Encapsulation	Dye adsorption	2
POM@MOF@SBA-15	$H_4[PMo_9V_3O_{40}] \cdot xH_2O$	MOF-199	–	1,3,5-trihydroxybenzene (BTC)	Encapsulation	Hydroxylation of benzene	3
POM@MIL101(Cr)	$H_3PW_{12}O_{40} \cdot xH_2O$	MIL101(Cr)	12~16	Terephthalate	Bottle-around-shipping	Esterification reaction	4
$Pd_{13}Se_8@MIL-101$	$[Pd_{13}Se_8O_{32}]^{6-} (Pd_{13}Se^-)$	MIL-101	12~16	–	Impregnation	Suzuki–Miyaura cross-coupling reaction	5
SRL-POM@MOF-199@MCM-41	$H_3PMo_6W_6O_{40}$	MOF-199 and MCM-41	–	1,3,5-benzenetricarboxylic (BTC)	Impregnation	Oxidative desulfurization	6
$PMoV_2@MIL-101$	$PMoV_2$	MIL-101	12~16	Terephthalic acid	Encapsulation	Aerobic Iodination of Arenes	7
ZZULI-1	$[W_{12}O_{40}]^{8-}$ and $[W_6O_{19}]^{2-}$	$Cu^{I}_2X_{2-bas edM}$	10	1,2,4,5-tetra(4-pyridyl)benzene (TPB)	Immobilization	Photocatalytic water splitting	8
$CoW_{12}@ZIF-8$	$K_6[CoW_{12}O_{40}] \cdot 6H_2O$	ZIF-8	–	2-methylimidazole	Encapsulation	Hydrogen evolution reaction	9
$Co_3O_4/CoMoO_4$	$H_3PMo_12O_{40} \cdot nH_2O$	ZIF-67	11.6	2-methylimidazole	Encapsulation	Hydrogen evolution reaction	10
H-POMOF	$H_3PW_{12}O_{40} \cdot xH_2O$	H-MOF	15.1~16.5	Benzene-1,3,5-tricarboxylic acid	Semi-encapsulation	Oxidative desulfurization (ODS)	This work

Table S5 Comparison of oxidative desulphurisation performance of recently reported representative POMOF matrix composites.

Catalyst	<i>n</i> (catalyst)	Sulfur compound	Conc. (ppm)	Oxidant	O / S	T (°C)	Time (min)	Conv. (%)	Ref.
PMo ₁₂ @NH ₂ -MIL-101(Cr)	4 mol/L	Real diesel	2300	H ₂ O ₂	6	50	120	80	11
ZIF-8@{Mo ₁₃ } ₂	0.15 g/L	DBT	500	TBHP	1	80	720	92	12
Mo ₁₁ V ₁	12 g/L	DBT	1000	H ₂ O ₂	1/2	70	50	90	13
Mo ₁₀ V ₂	12 g/L	DBT	1000	H ₂ O ₂	1/2	70	50	92	13
HPA@MOF@CA-3	1.8 g/L	Thiophene	1000	O ₂		25	180	84.91	14
HPA@MOF@CA-4	1.8 g/L	Thiophene	1000	O ₂		25	180	93.24	14
PTA@UiO-66	0.6mol %	BT	950	H ₂ O ₂	4	70	60	94.8	15
PTA@MIL-100(Fe)	0.6mol %	4,6-DMDBT	950	H ₂ O ₂	4	70	60	92.8	15
POM-PAF-1	8 g/L	DBT	500	H ₂ O ₂	6	30	30	98.5	16
SRL-1-POM@MOF-199@MCM-41	1.0 g/L	DBT	2000	O ₂		60	150	87.3	6
SRL-2-POM@MOF-199@MCM-41	1.0 g/L	DBT	2000	O ₂		60	150	92.8	6
SRL-4-POM@MOF-199@MCM-41	1.0 g/L	DBT	2000	O ₂		60	150	90.5	6
Fe ₃ O ₄ @UiO-66-PMoW	0.5 g/L	DBT	2000	O ₂		60	75	91.6	17
H-POMOF	3.5 g/L	DBT	500	H ₂ O ₂	5	60	150	98	This work

Table S6 Langmuir adsorption isotherm parameters at 50°C.

C_a	C_0	C_t	C_T	C_e	C_E	q_e	C_e/q_e
3.5	250	7.4	5.18	242.6	169.82	48.52	0.10676
	500	37	25.9	463	324.1	92.6	0.27969 8
	750	98.6	69.02	651.4	455.98	130.28	0.52978 2
	1000	338	236.6	662	463.4	132.4	1.78700 9

Table S7 Langmuir adsorption isotherm parameters at 60°C.

C_a	C_0	C_t	C_T	C_e	C_E	q_e	C_e/q_e
3.5	250	6.75	4.725	243.25	170.275	48.65	0.09712 2
	500	10	7	490	343	98	0.07142 9
	750	65.25	45.675	684.75	479.325	136.95	0.33351 6
	1000	303	212.1	697	487.9	139.4	1.52152 1

Table S8 Langmuir adsorption isotherm parameters at 70°C.

C_a	C_0	C_t	C_T	C_e	C_E	q_e	C_e/q_e
3.5	250	7.1	4.97	242.9	170.03	48.58	0.10230 5
	500	11	7.7	489	342.3	97.8	0.07873 2
	750	82.4	57.68	667.6	467.32	133.52	0.43199 5
	1000	322	225.4	678	474.6	135.6	1.66224 2

C_a —Adsorbent concentration (g/L)

C_0 —Initial sulfide concentration (ppm)

C_t —Equilibrium concentration (ppm)

C_T —Equilibrium concentration (mg/L)

C_e —Adsorbed concentration (ppm)

C_E —Adsorbed concentration (mg/L)

q_e —Adsorbent unit adsorption capacity (mg/g)

Table S9 Adsorption thermodynamic parameters at 50°C.

C_e (mg/L)	$K_d=q_e/C_e$	$\ln K_d$	ΔG (J/mol)
5.18	9.366795367	2.237171	-4778.17
25.9	3.575289575	1.274046	
69.02	1.887568821	0.63529	
236.6	0.559594252	-0.58054	

Table S10 Adsorption thermodynamic parameters at 60°C.

C_e (mg/L)	$K_d=q_e/C_e$	$\ln K_d$	ΔG (J/mol)
4.725	10.2962963	2.331784	-6419.741566
7	14	2.639057	
45.675	2.998357964	1.098065	
212.1	0.657237152	-0.41971	

Table S11 Adsorption thermodynamic parameters at 70°C.

C_e (mg/L)	$K_d=q_e/C_e$	$\ln K_d$	ΔG (J/mol)
4.97	9.774647887	2.279792	-6386.1
7.7	12.7012987	2.541704	
57.68	2.314840499	0.839341	
225.4	0.601597161	-0.50817	

Table S12 Cartesian Coordinates (A.U.) of POM by DFT.

NO	LB	ZA	FRAG	MASS	X	Y	Z
0	P	15.0000	0	30.974	2.253757	-0.972047	-2.458035
1	O	8.0000	0	15.999	-0.581771	-1.550797	-3.132544
2	O	8.0000	0	15.999	3.671425	-3.514408	-1.857107
3	O	8.0000	0	15.999	2.361763	0.803755	-0.077468
4	O	8.0000	0	15.999	3.565273	0.372731	-4.761686
5	W	14.0000*	0	183.85	0.624262	-0.185108	4.150262
6	W	14.0000*	0	183.85	0.475777	5.094995	0.194926
7	W	14.0000*	0	183.85	6.256770	2.430787	1.937837
8	W	14.0000*	0	183.85	8.187925	-3.896399	-0.658733
9	W	14.0000*	0	183.85	4.184969	-7.119554	-4.798246
10	W	14.0000*	0	183.85	2.553910	-6.515510	1.560741
11	W	14.0000*	0	183.85	-3.826011	1.615472	-4.264548
12	W	14.0000*	0	183.85	-2.042799	-4.258174	-6.675810
13	W	14.0000*	0	183.85	-3.679378	-3.660892	-0.309437
14	W	14.0000*	0	183.85	2.241268	4.442165	-6.657478
15	W	14.0000*	0	183.85	4.028446	-1.435701	-9.061506
16	W	14.0000*	0	183.85	8.022669	1.788864	-4.917272
17	O	8.0000	0	15.999	-5.252176	-0.702595	-1.805565
18	O	8.0000	0	15.999	-3.888297	-5.178724	-3.643854
19	O	8.0000	0	15.999	-2.216481	-1.506930	2.259613
20	O	8.0000	0	15.999	-0.875297	-5.873343	0.458507
21	O	8.0000	0	15.999	-3.999235	-1.157346	-6.657692
22	O	8.0000	0	15.999	-2.349909	3.536422	-1.523261
23	O	8.0000	0	15.999	-1.131582	3.087447	-6.257065
24	O	8.0000	0	15.999	0.573870	-2.527285	-8.556037
25	O	8.0000	0	15.999	0.681488	-6.455440	-5.611757
26	O	8.0000	0	15.999	6.174022	-5.944366	1.627430
27	O	8.0000	0	15.999	7.418415	-6.405438	-3.221107
28	O	8.0000	0	15.999	3.124572	-8.406023	-1.530533
29	O	8.0000	0	15.999	7.488614	-0.978424	1.435587

30	O	8.0000	0	15.999	8.689687	-1.426749	-3.303796
31	O	8.0000	0	15.999	4.873273	-4.501213	-7.256893
32	O	8.0000	0	15.999	4.004642	1.183628	4.547336
33	O	8.0000	0	15.999	-0.402769	3.210816	3.217267
34	O	8.0000	0	15.999	3.891051	5.204810	1.527406
35	O	8.0000	0	15.999	1.845875	5.484034	-3.172827
36	O	8.0000	0	15.999	2.091792	-3.480546	3.551415
37	O	8.0000	0	15.999	5.881030	4.479748	-6.191961
38	O	8.0000	0	15.999	2.834073	2.020403	-9.346967
39	O	8.0000	0	15.999	7.241656	-0.003831	-8.021172
40	O	8.0000	0	15.999	7.364326	2.947546	-1.512323
41	O	8.0000	0	15.999	2.190819	-8.893360	3.763216
42	O	8.0000	0	15.999	-3.565509	-6.007430	-8.969298
43	O	8.0000	0	15.999	-6.180216	-5.072096	1.236896
44	O	8.0000	0	15.999	-0.395998	-0.376263	7.242193
45	O	8.0000	0	15.999	8.631956	3.824066	3.685909
46	O	8.0000	0	15.999	-0.631779	8.081441	0.896836
47	O	8.0000	0	15.999	-6.424713	3.400524	-5.100528
48	O	8.0000	0	15.999	1.734626	7.203860	-8.317287
49	O	8.0000	0	15.999	11.01042 2	2.947699	-5.524275
50	O	8.0000	0	15.999	11.23147 5	-4.704798	0.191002
51	O	8.0000	0	15.999	4.822924	-9.863655	-6.441495
52	O	8.0000	0	15.999	4.611640	-2.217451	-12.173926

Table S13 Mayer Population Analysis of POM by DFT.

ATOM	NA	ZA	QA	VA	BVA	FA
0 P	13.6543	15.0000	1.3457	4.9293	4.9293	-0.0000
1 O	8.6307	8.0000	-0.6307	2.0446	2.0446	0.0000
2 O	8.6320	8.0000	-0.6320	2.0431	2.0431	-0.0000
3 O	8.6320	8.0000	-0.6320	2.0428	2.0428	-0.0000
4 O	8.6320	8.0000	-0.6320	2.0424	2.0424	-0.0000
5 W	12.6857	14.0000	1.3143	6.4591	6.4591	0.0000
6 W	12.6878	14.0000	1.3122	6.4605	6.4605	0.0000
7 W	12.6857	14.0000	1.3143	6.4592	6.4592	0.0000
8 W	12.6869	14.0000	1.3131	6.4601	6.4601	0.0000
9 W	12.6860	14.0000	1.3140	6.4591	6.4591	-0.0000
10 W	12.6862	14.0000	1.3138	6.4595	6.4595	0.0000
11 W	12.6858	14.0000	1.3142	6.4597	6.4597	0.0000
12 W	12.6876	14.0000	1.3124	6.4611	6.4611	0.0000
13 W	12.6880	14.0000	1.3120	6.4616	6.4616	0.0000
14 W	12.6864	14.0000	1.3136	6.4598	6.4598	-0.0000
15 W	12.6866	14.0000	1.3134	6.4595	6.4595	-0.0000
16 W	12.6861	14.0000	1.3139	6.4592	6.4592	-0.0000
17 O	8.5618	8.0000	-0.5618	2.2645	2.2645	0.0000
18 O	8.5619	8.0000	-0.5619	2.2645	2.2645	-0.0000
19 O	8.5827	8.0000	-0.5827	2.2432	2.2432	-0.0000
20 O	8.5825	8.0000	-0.5825	2.2432	2.2432	-0.0000
21 O	8.5612	8.0000	-0.5612	2.2653	2.2653	0.0000
22 O	8.5830	8.0000	-0.5830	2.2427	2.2427	-0.0000
23 O	8.5828	8.0000	-0.5828	2.2432	2.2432	0.0000
24 O	8.5828	8.0000	-0.5828	2.2429	2.2429	0.0000
25 O	8.5829	8.0000	-0.5829	2.2428	2.2428	-0.0000
26 O	8.5617	8.0000	-0.5617	2.2646	2.2646	0.0000
27 O	8.5615	8.0000	-0.5615	2.2651	2.2651	0.0000
28 O	8.5618	8.0000	-0.5618	2.2646	2.2646	-0.0000
29 O	8.5832	8.0000	-0.5832	2.2426	2.2426	0.0000

30 O	8.5826	8.0000	-0.5826	2.2432	2.2432	-0.0000
31 O	8.5827	8.0000	-0.5827	2.2431	2.2431	-0.0000
32 O	8.5616	8.0000	-0.5616	2.2649	2.2649	0.0000
33 O	8.5619	8.0000	-0.5619	2.2645	2.2645	0.0000
34 O	8.5616	8.0000	-0.5616	2.2649	2.2649	-0.0000
35 O	8.5827	8.0000	-0.5827	2.2430	2.2430	-0.0000
36 O	8.5828	8.0000	-0.5828	2.2431	2.2431	0.0000
37 O	8.5616	8.0000	-0.5616	2.2648	2.2648	-0.0000
38 O	8.5616	8.0000	-0.5616	2.2648	2.2648	-0.0000
39 O	8.5618	8.0000	-0.5618	2.2647	2.2647	0.0000
40 O	8.5831	8.0000	-0.5831	2.2428	2.2428	-0.0000
41 O	8.3204	8.0000	-0.3204	2.4524	2.4524	0.0000
42 O	8.3206	8.0000	-0.3206	2.4519	2.4519	-0.0000
43 O	8.3205	8.0000	-0.3205	2.4520	2.4520	0.0000
44 O	8.3204	8.0000	-0.3204	2.4525	2.4525	0.0000
45 O	8.3204	8.0000	-0.3204	2.4525	2.4525	-0.0000
46 O	8.3206	8.0000	-0.3206	2.4518	2.4518	-0.0000
47 O	8.3205	8.0000	-0.3205	2.4525	2.4525	0.0000
48 O	8.3206	8.0000	-0.3206	2.4522	2.4522	0.0000
49 O	8.3205	8.0000	-0.3205	2.4523	2.4523	0.0000
50 O	8.3205	8.0000	-0.3205	2.4521	2.4521	-0.0000
51 O	8.3205	8.0000	-0.3205	2.4523	2.4523	-0.0000
52 O	8.3205	8.0000	-0.3205	2.4521	2.4521	-0.0000

NA - Mulliken gross atomic population

ZA - Total nuclear charge

QA - Mulliken gross atomic charge

VA - Mayer's total valence

BVA - Mayer's bonded valence

FA - Mayer's free valence

Reference

1. Q. Lan, Z. M. Zhang, C. Qin, X. L. Wang, Y. G. Li, H. Q. Tan and E. B. Wang, *Chemistry–A European Journal*, 2016, **22**, 15513-15520.
2. M. Huo, W. Yang, H. Zhang, L. Zhang, J. Liao, L. Lin and C. Lu, *RSC Adv.*, 2016, **6**, 111549-111555.
3. H. Yang, J. Li, H. Zhang, Y. Lv and S. Gao, *Microporous and mesoporous materials*, 2014, **195**, 87-91.
4. J. Juan-Alcañiz, E. V. Ramos-Fernandez, U. Lafont, J. Gascon and F. Kapteijn, *Journal of Catalysis*, 2010, **269**, 229-241.
5. S. Bhattacharya, W. W. Ayass, D. H. Taffa, T. Nisar, T. Balster, A. Hartwig, V. Wagner, M. Wark and U. Kortz, *Inorg. Chem.*, 2020, **59**, 10512-10521.
6. S.-W. Li, Z. Yang, R.-M. Gao, G. Zhang and J.-s. Zhao, *Applied Catalysis B: Environmental*, 2018, **221**, 574-583.
7. J. Sun, H. S. Jena, S. Abednatanzi, Y.-Y. Liu, K. Leus and P. Van Der Voort, *ACS Applied Materials & Interfaces*, 2022, **14**, 37681-37688.
8. D. Shi, R. Zheng, C.-S. Liu, D.-M. Chen, J. Zhao and M. Du, *Inorg. Chem.*, 2019, **58**, 7229-7235.
9. Y. Song, Y. Peng, S. Yao, P. Zhang, Y. Wang, J. Gu, T. Lu and Z. Zhang, *Chinese Chemical Letters*, 2022, **33**, 1047-1050.
10. L. Zhang, T. Mi, M. A. Ziaee, L. Liang and R. Wang, *Journal of Materials Chemistry A*, 2018, **6**, 1639-1647.
11. C. M. Granadeiro, P. M. Ferreira, D. Julião, L. A. Ribeiro, R. Valença, J. C. Ribeiro, I. S. Gonçalves, B. De Castro, M. Pillinger and L. Cunha-Silva, *Energies*, 2018, **11**, 1696.
12. M. Ghahramaninezhad, F. Pakdel and M. N. Shahrak, *Polyhedron*, 2019, **170**, 364-372.
13. P. Wei, Y. Yang, W. Li and G. Li, *Fuel*, 2020, **274**, 117834.
14. J. Li, Z. Yang, G. Hu and J. Zhao, *Chemical Engineering Journal*, 2020, **388**, 124325.
15. X. S. Wang, L. Li, J. Liang, Y. B. Huang and R. Cao, *ChemCatChem*, 2017, **9**, 971-979.
16. P. Wang, L. Jiang, X. Zou, H. Tan, P. Zhang, J. Li, B. Liu and G. Zhu, *ACS applied materials & interfaces*, 2020, **12**, 25910-25919.

17. S.-W. Li, H.-Y. Zhang, T.-H. Han, W.-Q. Wu, W. Wang and J.-S. Zhao, *Separation and Purification Technology*, 2021, **264**, 118460.